ACS APPLIED MATERIALS & INTERFACES
Research Article
Cite This: ACS Appl. Mater. Interfaces 2019, 11, 11928−11935
www.acsami.org

Downloaded via UNIV OF GLASGOW on July 12, 2020 at 19:55:11 (UTC).
See https://pubs.acs.org/sharingguidelines for options on how to legitimately share published articles.

Capacitive Pressure Sensor with Wide-Range, Bendable, and High Sensitivity Based on the Bionic Komochi Konbu Structure and Cu/Ni Nanofiber Network

Jian Wang,[†] Ryuki Suzuki,[†] Marine Shao,[‡] Frédéric Gillot,[‡] and Seimei Shiratori*,[†]

[†]Center for Material Design Science, School of Integrated Design Engineering, Keio University, 3-14-1 Hiyoshi, Yokohama 223-8522, Japan

[‡]LTDS UMR CNRS 5513—DySCo Team/ECL, 36 av., Guy de Collongue, 69134 Ecully Cedex, France

Supporting Information

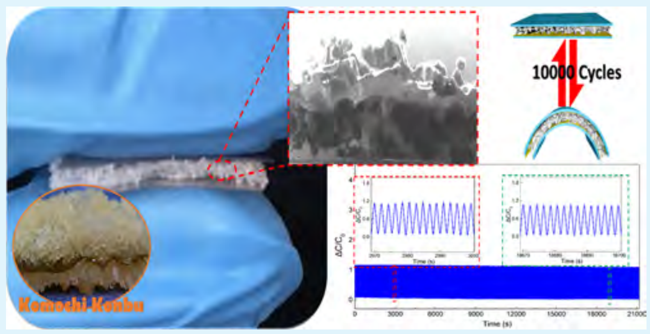

ABSTRACT: High-performance flexible pressure sensors have an essential application in many fields such as human detection and human−computer interaction. Herein, on the basis of the dielectric layer of a bionic komochi konbu structure, we propose a low-cost and novel capacitive sensor that achieves high sensitivity and stability over a broad range of tactile pressures. Further, the flexible and durable electrode layer of the transparent junctionless copper/nickel-nanonetwork was prepared based on electrospinning and electroless deposition techniques, which ensured high bending stability and high cycle stability of our sensor. More importantly, because of the sizeable protruding structure and internal micropores in the elastomer structure we designed, the inward curling of the protruding structure and the effectual closing of the micropores increase the effective dielectric constant under the action of the compressive force, improving the sensitivity of the sensor. Measured response and relaxation time (162 ms) are 250 times faster than those of a conventional flat polydimethylsiloxane capacitive sensor. In addition, the fabricated capacitive pressure sensor demonstrates the ability to be used on wearable applications, not only to quickly recognize the tapping and bending of a finger but also to show that the pressure of the finger can be sensed when the finger grabs the object. The sensors we have developed have shown great promise in practical applications, such as human rehabilitation and exercise monitoring, as well as human−computer interaction control.

KEYWORDS: *capacitive pressure sensor, electrospinning, capacitive sensor, wearable devices, human motion*

INTRODUCTION

Highly sensitive flexible tactile sensors have attracted extensive attention because of their flexible and folding characteristics, which can be perfectly applied to the complex 3D surface of daily used objects. Because of the broad application prospect of sensors, they became a new research field. Recent significant progress in sensor materials, manufacturing processes, and sensor structures made various new applications achievable. For example, in the field of bionic robots,[1,2] the attachment of flexible sensors to the robot's skin can enable the robot to perceive the external environment, which is more conducive to control the robot for complex tasks and realize the application of human interaction.[3,4] In the field of intelligent medical[5−7] and motion detection,[8−10] a flexible sensor can be directly attached to the human skin as an E-skin,[11−13] and multiple health indicators such as pulse,[14,15] blood sugar concentration,[13,16] and the amount of exercise[17−19] can be collected, which are of great significance for human health detection and disease diagnosis. Different sensing mechanisms such as capacitance,[20−22] piezoelectric,[23,24] piezoresistive,[10,25−27] field effect transistor,[24,28] and optics[29] have been intensely studied to prepare flexible sensors with high performance, friendly to the human body and stable. In particular, the capacitive sensor has become the preferred type of high-sensitivity sensor because of its excellent sensitivity, low power consumption, outstanding temperature insensitivity,[30] and rapid dynamic response.[31,32]

In principle, the capacitive pressure sensors currently under study can be considered as parallel plate capacitors. This type of capacitor is usually composed of two flexible electrodes at the top/bottom and a flexible dielectric in between.[33] The capacitance of the parallel plate capacitor is proportional to the dielectric constant and the corresponding overlapping surface of the two electrodes and inversely proportional to the distance between the plate electrodes.[34] When the sensor is applied by an external force, the thickness of the capacitive sensor decreases accordingly, which in turn causes a change in capacitance. The amount of external pressure applied can be

Received: January 15, 2019
Accepted: March 4, 2019
Published: March 4, 2019

© 2019 American Chemical Society

DOI: 10.1021/acsami.9b00941
ACS Appl. Mater. Interfaces 2019, 11, 11928−11935

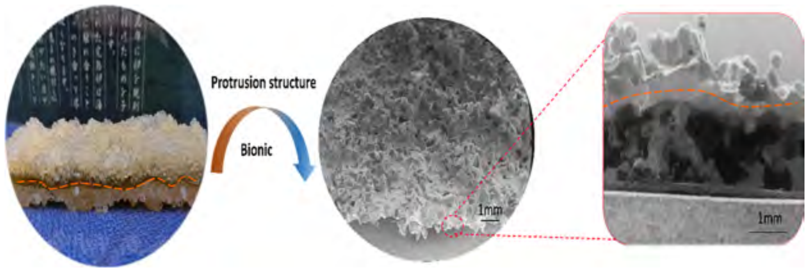

Figure 1. Comparison of komochi konbu with the designed bionic structure.

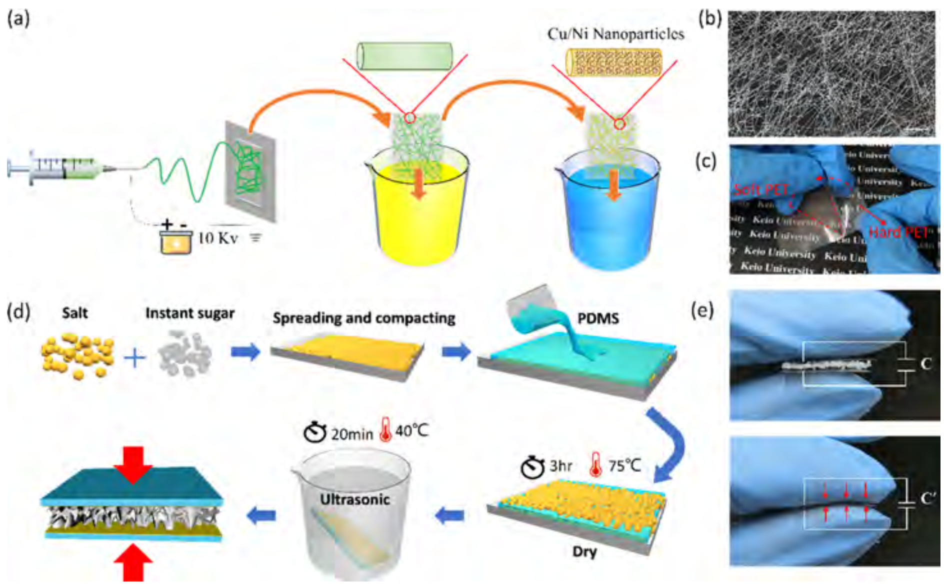

Figure 2. (a) Schematic diagram of the manufacturing process of the Cu/Ni nanofiber flexible electrode of the sensor. (b) SEM image of Cu/Ni nanofiber flexible electrode. (c) Photograph of the peeled part of the hard substrate of the Cu/Ni nanofiber flexible electrode. (d) Schematic diagram of preparation of BKKE dielectric layer of the sensor. (e) Actual photograph of the sensor and the principle of pressure action.

obtained by monitoring the print of these capacitive signals. Although this parallel plate capacitor-based performance has high stability, the change of capacitance is small, and the sensitivity is very low, which cannot meet the current sensor performance requirements. Therefore, most studies focus on improving the sensitivity of the sensors mainly through the microstructure of the electrode surface and dielectric layer. The fabrication of microstructure electrodes usually requires complex molds and time-consuming transfer processes, of which patterns are mostly obtained by photolithography,[6,35] dip-coating,[36,37] and chemical etching.[38] Given the high cost and complicated production process, it is difficult to obtain a large-scale application. Recently, some new preparation methods have also appeared, such as Su et al.,[39] used the leaf structure of mimosa to prepare a flexible pressure sensor, and the pressure detection range was 0−1.5 kPa. Shuai et al.[33] used the surface of the prestretched polydimethylsiloxane (PDMS) film coated with silver nanowires, the PDMS film formed a buckling structure during the relaxation process, and the prepared capacitive sensor operates at a pressure range of less than 6.7 kPa. All of these methods can enhance the sensitivity of the sensor, but we should note that their working range is limited to the pressure range of 10 kPa, whereas the pressure range of wearable devices in daily applications is generally from 1 to 100 kPa.[40] Therefore, these sensors are not well suited for the application of most wearable devices.

Another method has also been studied in the selection and preparation of dielectric layers for microstructures. For example, He et al.[41] used a nylon mesh as a dielectric layer to prepare a capacitive sensor. Kang et al.[22] developed a sponge-like structure of a thin-film dielectric layer in combination with an ITO film to produce a high-sensitivity capacitive pressure sensor. Song et al.[42] used a method of leaching sugar cubes to prepare a silicone elastomer with a microporous structure, but the dielectric layer thickness was generally at 10 mm because of the limitation of the template, making the sensor not flexible enough to make a wearable electronic device, the sensor itself must be flexible, sensitive, and stable. Therefore, the design and preparation of a dielectric layer elastomer with excellent performance, combined with a flexible conductive network electrode layer, are necessary conditions for the preparation of flexible and durable wearable flexible sensors.

In view of the above requirements, we propose a flexible capacitive sensor based on a bionic komochi konbu structure elastomer (BKKE), which can not only improve the flexibility of the sensor but also enhance the performance of the sensor (Figure 1). "Komochi konbu" is a traditional Japanese food with herring eggs attached to kelp, herring is instinctively laying eggs on the surface of kelp which is a unique double-sided heterogeneous structure, as shown in Figure S1. The device consists of a Cu/Ni nanofiber network prepared on a particularly flexible polyester (PET) film as top and bottom

DOI: 10.1021/acsami.9b00941
ACS Appl. Mater. Interfaces 2019, 11, 11928−11935

electrodes, and the electrodes were coupled with BKKE as dielectric layers. We designed a BKKE dielectric layer by mixing the instant sugar powder and salt particles as a sacrificial layer, and prespinning the PDMS elastomer on the template before they were placed face to face. The thin film-like microstructure of the dielectric layer provides a higher base capacitance, making it easier for the sensor to exhibit capacitance changes. Furthermore, under the pressure of 100 kPa, the sensor still has an ultrafast recovery speed of 162 ms and excellent mechanical stability and additionally, benefits from Cu/Ni nanofiber with the softness and high conductivity, assembled with a BKKE dielectric layer to form a flexible capacitive sensor with excellent performance, which can not only have a wide pressure detection range but also detect bending and distortion. It is a competitive candidate for artificial electronic skin and wearable devices.

■ RESULTS AND DISCUSSION

The manufacturing process of flexible capacitive sensor based on Cu/Ni nanofibers and BKKE dielectric layers is shown in Figure 2. The preparation process can be mainly divided into the following 3 steps: (1) preparing a nanofiber mesh electrode layer on the surface of the flexible PET, (2) preparation of a BKKE as a dielectric layer by a composite stencil of sugar and salt crystals, and (3) forming a reliable capacitive sensor with the electrode layer and the dielectric layer (Figure S2, Supporting Information). Figure 2a describes the fabrication of a Cu/Ni nanonetwork in detail. The prepared polyvinyl butyral/$SnCl_2$ nanofiber network was deposited directly on the surface of the composite double-layer PET film by electrospinning. The surface of the prepared nanonetwork was then catalyzed in an activation solution of $PdCl_2$. After rinsing with deionized water, placed it in a 65 °C Cu/Ni plating solution for 5 min. Figure 2b shows an scanning electron microscopy (SEM) image of a Cu/Ni electroless nanofiber network. The flexible PET film was directly peeled off from the composite PET film for use in the electrode portion of the sensor (Figure 2c), and it was also observed that the prepared nanomesh had excellent transparency. Figure 2d shows the method of preparing a BKKE dielectric layer. The instant sugar and the salt crystals were mixed with a small amount of water, poured into a mold to prepare a template, and dried at 70° C for 1 h. The PDMS liquid, from which the bubbles have been removed, was spin-coated on the surface of the template, and the overall thickness of the dielectric layer can be adequately controlled by the time and speed of spin coating. Then, the PDMS liquid was covered with another salt crystal template, and they were gently pressed and placed in an oven at 75 °C for 3 h. The double-sided BKKE was obtained by setting the cured PDMS in an ultrasonic cleaning bath for 20 min. Because of the uneven structure on the surface of the salt crystal stencil and the tiny gap between the salt crystal particles, and then under the action of gravity, PDMS can immerse into these voids and concave structures, eventually forming a BKKE composite structure (Figure S3, Supporting Information). The actual photograph of the sensor and the principle of pressure action is shown in Figure 2e. Further, to intuitively know the thickness of the sensor, the sensor is compared with 500 yen as shown in Figure S4. It can be seen from the figure that the overall thickness of the prepared sensor is about 2 mm. The surface 3D structure and multiview detail of the BKKE dielectric layer in the sensor are shown in Figures S5 and S6. The figures clearly show the surface details of the bionic komochi konbu structure. Like the surface of komochi konbu, it has a multilayered convex and concave structures that form a rich surface structure.

The primary evaluation indicators of the pressure sensor performance are sensitivity, response time, detection limit, and working stability. Sensitivity is a decisive factor in evaluating the sensor performance. Different dielectric layer sensors from BKKE and nonporous (flat) were tested, respectively. Figure 3a shows the capacitive response curves of the pressure sensor of different BKKEs based on proportions of soluble sugar and salt (1:5, 1:7, 1:9, and 1:11) and a flat PDMS dielectric layer. The sensitivity can be defined here as the ratio $S = \delta(\Delta C/C_0)/\delta p$, where p is the pressure applied to the sensor, ΔC and C_0 are the capacitance of the relative change and capacitance without the applied force, respectively. From the capacitive pressure sensor, it is evident that the BKKE is used as the dielectric layer to significantly enhance the sensitivity of the sensor, and the BKKE dielectric layer (the ratio of instant soluble sugar to salt particles is 1:9) has better sensitivity. First, in the pressure range from 0 to 5 kPa, although the capacitive pressure sensor with flat PDMS has the pressure sensitivity of 8.35×10^{-3} kPa^{-1}, the capacitive pressure sensor consisting of a BKKE (1:9) as the dielectric layer has the sensitivity of 1.71×10^{-1} kPa^{-1}, as shown in Figure 3a. When the pressure applied to the sensor is greater than 50 kPa, the sensitivity of the capacitive sensor composed of the BKKE (1:9) as the dielectric layer can still reach 9.80×10^{-3} kPa^{-1}, while the sensitivity of the sensor with the flat PDMS as the dielectric layer is the only 5.65×10^{-4} kPa^{-1}. It shows that our sensor still has excellent sensitivity and practicability under considerable stress. Table S1 shows the specific sensitivity of the pressure sensor of BKKE based on different proportions of soluble sugar and salt (1:5, 1:7, 1:9 and 1:11) and a flat PDMS dielectric layer. This is because by changing the ratio of instant sugar (binder) to salt particles, we found that BKKE structures with different surface structures were formed. As shown in Figure S7, the instant sugar melts quickly upon contact with water, and the salt particles are mostly unable to melt because of the small amount of water so that the instant sugar can solidify the salt particles. By adjusting the proportion of instant sugars, the bonding between the salt particles will be different. Because of the binder action of the instant sugar, there is no void between the salt particles adhered by the instant sugar, and a gap is formed between the salt particles not adhered by the instant sugar for immersion of the PDMS to form a special

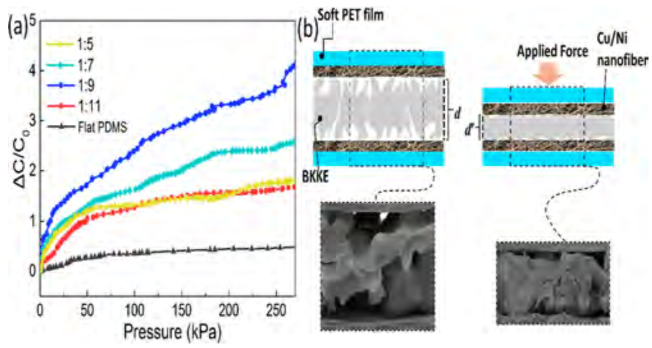

Figure 3. (a) Pressure−capacitance curve of BKKE pressure sensor based on different proportions of instant sugar and salt (1:5, 1:7, 1:9 and 1:11), and a flat PDMS dielectric layer. (b) The working principle of BKKE dielectric layer and SEM images before and after pressure.

DOI: 10.1021/acsami.9b00941
ACS Appl. Mater. Interfaces 2019, 11, 11928−11935

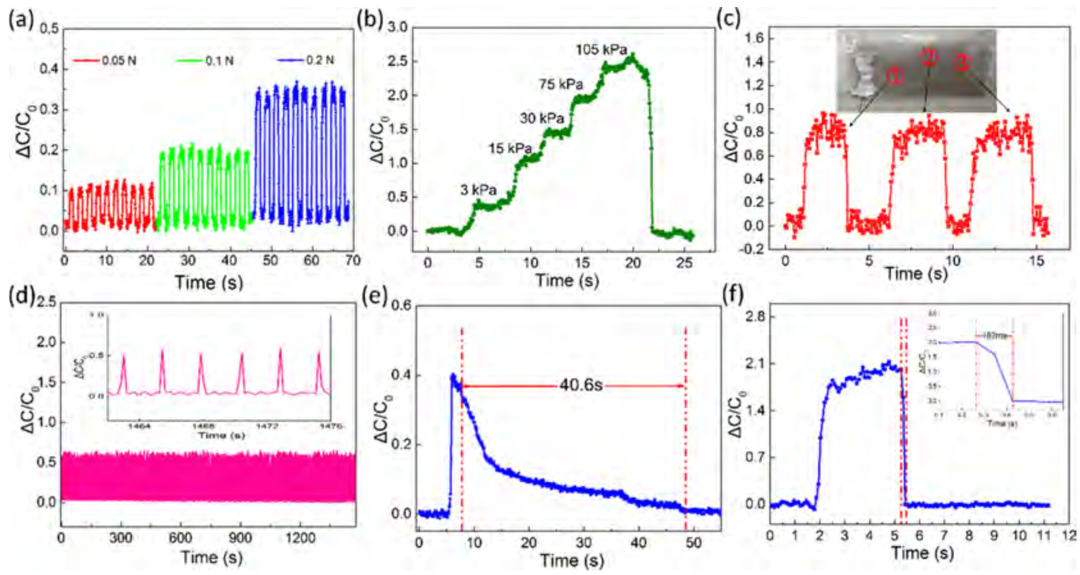

Figure 4. (a) Capacitance response of BKKE-based pressure sensors at different pressures. (b) Capacitance response of BKKE-based pressure sensors under stepped loading–unloading pressure. (c) Capacitance signal of the pressure sensor under the same pressure at different pressure locations. (d) Stability of the BKKE-based capacitive sensor response after 1000 cycles of continuous tapping of the sensor and the inset is a partially enlarged view of 6 cycles therein. (e) Recovery time curve based on flat PDMS pressure sensor. (f) Recovery time curve based on BKKE dielectric layer pressure sensor.

komochi konbu structure surface. However, the proportion of salt particles is too large to form a large number of voids for PDMS to immerse, thereby forming an aggregation effect of the surface protrusion structure and reducing the air content contained in the structure, thus reducing the sensitivity of the BKKE-based dielectric layer sensor. At the same time, we noticed that the response curve of the sensor is not a simple linear relationship but a linear response with multiple levels of variation. The reason for this phenomenon is mainly due to the designed komochi konbu structure, as shown in Figure S8. When the pressure is applied, the part in contact with the nanofiber electrode will be stressed first, and then, the internal protrusion structure will be stressed, which will have multilevel stress. Therefore, the response curve presented by the sensor is not a direct and simple linear relationship but a multilevel linear relationship curve.

For ease of understanding, the pressure-sensing mechanism between the sensors of conventional plate dielectric and BKKE dielectric is analyzed, as shown in Figure 3b. When the BKKE capacitance sensor is not under pressure, the protrusion of the BKKE is in active contact with the electrode of the Cu/Ni nanofiber network between the upper and lower layers (Figure S9, Supporting Information). Therefore, there are a large number of air gaps in the capacitor structure. With only the flat PDMS, there is almost no excess space in the sensor with a flexible PET (Figure S10, Supporting Information). Because the Poisson's ratio of PDMS is 0.47,[33,41] the capacitance sensor A remains almost unchanged, so when the sensor is under pressure, the capacitance change of the sensor depends mainly on the shift of d and ε. At the same time, it is considered that these bionic komochi konbu structures can be gradually bent inward and closed under the action of pressure, which also improves the effective dielectric constant because of air displacement.[40]

The capacitance of the sensor without pressure (C_0) and with pressure (C) of the sensor can be expressed as

$$C_0 = \varepsilon_0 \varepsilon_{r0} \frac{A}{d} \tag{1}$$

$$C = \varepsilon_0 \varepsilon_r \frac{A}{d'} \tag{2}$$

where A is the electrode area, d and d' are the thickness of the dielectric without and with applied pressure, respectively, ε_0 is the dielectric constant of the vacuum, and ε_{r0} and ε_r are the relative permittivity of the dielectric without and with pressure, respectively. Accordingly, the capacitance change can be calculated by

$$\frac{\Delta C}{C_0} = \frac{C - C_0}{C_0} = \frac{\varepsilon_r}{\varepsilon_{r0}} \cdot \frac{d}{d'} - 1 \tag{3}$$

For the sensor with a BKKE dielectric layer, $\varepsilon_r > \varepsilon_{r0}$, because of the increase in the relative volume of PDMS elastomer. Therefore, as the dielectric constant increases, its capacitance change increases, and the sensitivity increases accordingly.

To evaluate the responsiveness and repeatability of the prepared flexible sensor, the response performance of the sensor under different pressures was investigated, as shown in Figure 4a. The results show that the sensor has a stable capacitive response under various loads, and high sensitivity, excellent repeatability and can quickly return to its initial state when the loaded pressure was removed. Through further step pressure test, it can be seen that the sensor has a corresponding capacitive response according to the difference of the step pressure, showing outstanding pressure recognition performance, as shown in Figure 4b. At the same time, the different positions of the sensor were also tested by the applied pressure, and the capacitance response remained stable, indicating that the location of the sensor did not differ from the force (Figure 4c). To further evaluate and sense the actual behavior of the object on the sensor, a weight of 10 g was placed vertically and horizontally on the pressure sensor, respectively, triggering two distinct capacitive signal responses, as shown in Figure S11. Because the area of the sensor in contact with the weight

DOI: 10.1021/acsami.9b00941
ACS Appl. Mater. Interfaces 2019, 11, 11928−11935

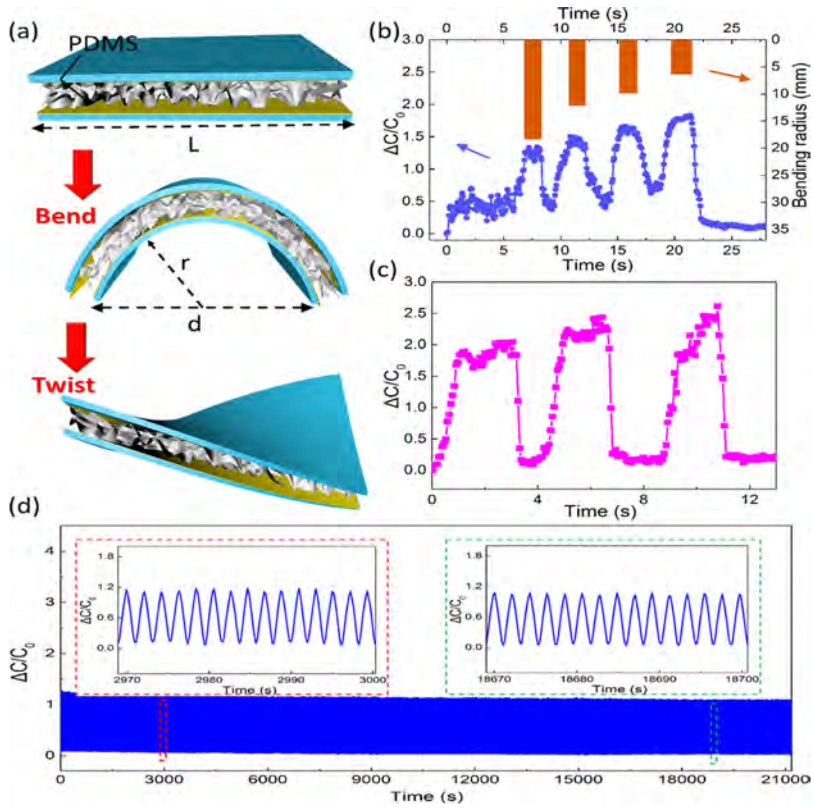

Figure 5. (a) Schematic diagram of the bending and twisting of the BKKE sensor. (b) Capacitance response diagram of BKKE sensor under different bending radius. The left axis is the capacitive response curve, and the right axis is the bend radius. (c) Capacitance response of sensor under torsion. (d) Stability and durability of the response of the sensor after 10 000 bending cycles and the two insets are magnified cycles of different time periods.

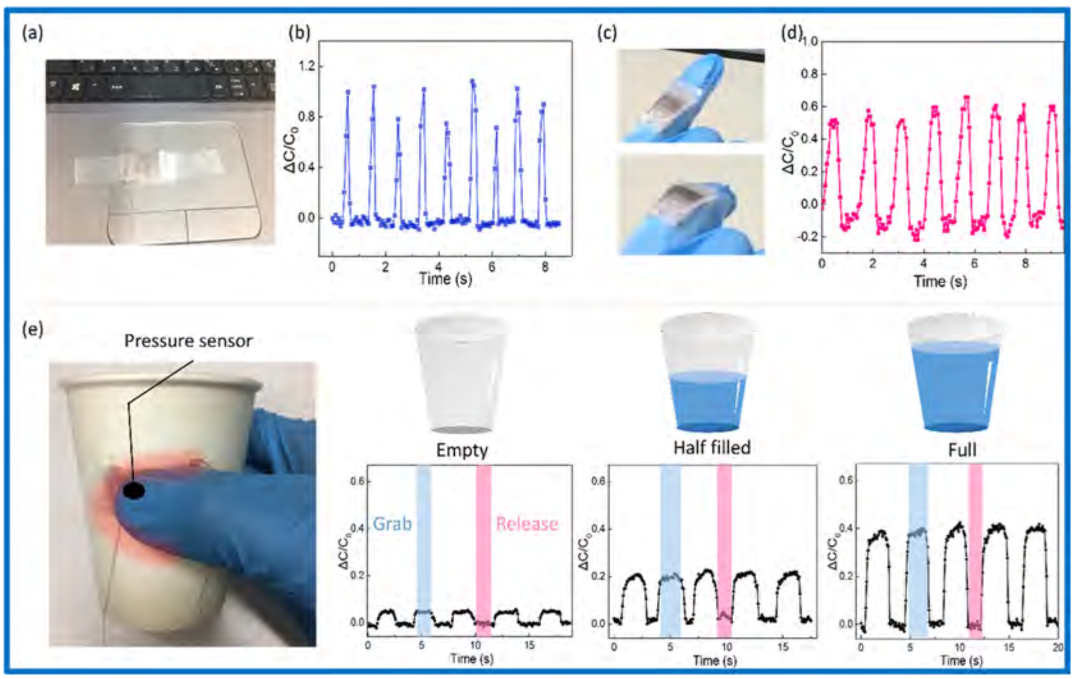

Figure 6. (a) Photograph of the sensor attached to the touchpad of the laptop. (b) Capacitance response diagram when the finger clicks on the sensor. (c) Photograph of the sensor attached to the joint of the index finger. (d) Real-time monitoring of pressure sensors for finger bending. (e) Capacitance response of sensor located between the thumb and the paper cup when catching objects of different weights.

changes, the compressed area and compression amplitude of the sensor are different when placed on the sensor. Figure 4d shows that the prepared pressure sensor also has a long cycle life. The sensor was tapped 1000 times in the same position. During the test, the relative capacitance change of the sensor remained stable. The recovery times of BKKE sensors and

DOI: 10.1021/acsami.9b00941
ACS Appl. Mater. Interfaces 2019, 11, 11928−11935

conventional flat PDMS sensors were compared under 100 kPa pressure (Figure 4e,f). We can clearly understand from the picture that the conventional flat PDMS sensor takes about 40.6 s to recover to the initial state after removing the external force, whereas the BKKE sensor only takes 162 ms. Thanks to the particular dielectric elastomer structure of the BKKE sensor, with the flat PDMS as the dielectric layer, there is just a small gap between the PDMS and the flexible electrode, combined with the viscoelasticity of the flat PDMS itself, so this process requires about 250 times more time than the BKKE sensor.

A schematic of the bending and twisting test is shown in Figure 5a. The two ends of the sensor were fixed on the rigid PET substrate, pushing one end of the sensor to the required bending radius and twisting at the center of the sensor to test the capacitive response of the sensor. Figure 5b shows the curve of bending curvature and sensor capacitance changing with time. The calculation formula of the bending radius is shown in Figure S12 (the Supporting Information). We can see that the capacitance of the sensor has a negative correlation with the radius of curvature. It also means that the BKKE sensor with the Cu/Ni nanofiber membrane as the electrode has excellent bending properties. In the application of the sensor, not only excellent bending properties but also the reliable torsional stability of the sensor are required. Thus, the same amount of twist was repeatedly applied to the sensor multiple times, measuring the real-time $\Delta C-t$ plot and displaying it in Figure 5c. The results indicate that the sensor has no noticeable change in capacitance under the torsion, showing the robust distortion stability of the sensor. As shown in Figure 5d, the relative capacitance response curve of the capacitive sensor shows excellent stability and durability after 10 000 cycles of bending.

Fast response speed and excellent sensitivity ensure that the sensor is suitable for the response of computer touchpad buttons. Figure 6a shows the prepared sensor placed on a laptop touchpad. Figure 6b shows a stable and synchronized response to a finger click based on a BKKE sensor. In addition, the sensor can quickly identify clicks and double-clicks; the time interval was only a few hundred microseconds, as shown in Figure S13 (the Supporting Information). The prepared sensor is a promising material in wearable platforms. For demonstration, exercise performance can be monitored by mounting BKKE sensor on different parts of the body, such as finger joints. In Figure 6c, the sensor is mounted on the index finger joint of a blue rubber glove for detecting the bending and stretching of the finger. Figure 6d shows the relative capacitance response of the sensor during the bending and stretching of the finger. The results show that the sensor can react quickly and repeatedly to finger movements when the finger is bent at a specific amplitude and frequency. During a grasping experiment, the subjects grasped and released paper cups five times of different weights (4.7, 85.8, and 163.2 g) while recording the capacitance signal of the sensor (Figure 6e). When the subject grasps the empty paper cup, the capacitance value changes minimally, and as the weight of the water in the paper cup increases, the capacitance value varies significantly. The results show that the prepared sensor can be used to sense the pressure of the fingertip during a finger gripping action. Therefore, the prepared BKKE sensor can be used for human body rehabilitation and exercise monitoring, as well as human−computer interaction control.

■ CONCLUSION

We have designed and manufactured a wearable capacitive pressure sensor based on a jointless Cu/Ni nanofiber mesh and BKKE as a dielectric layer, which has high ultrasensitivity and excellent stability within a wide pressure range and which adopts a low-cost, efficient, and straightforward preparation process. Elastomers of double-sided BKKE structure were prepared using solid particles of instant sugar and salt crystals with high deformation and recovery capabilities. In addition, because of the sizeable protruding structure and internal micropores in the elastomer structure we designed, the inward curling of the protruding structure and effectual closing of the micropores increase the effective dielectric constant under the action of the compressive force, increasing the sensitivity of the sensor. More importantly, the sensor has an ultrafast response and recovery time (162 ms), which is 250 times faster than a conventional flat PDMS capacitive sensor (40.6 s). To study the applicability of the better wearable device, it is proved that the BKKE sensor can be easily used as a wearable sensor device, which not only can quickly recognize the tapping and bending of the finger but also shows the ability of the sensor to sense the pressure of the thumb while grasping the objects. We believe that this low-cost, excellent stability, and dynamic monitoring capability is ideal for areas such as rehabilitation, physical activity, and human−computer interaction control.

■ EXPERIMENTAL SECTION

Preparation of BKKE Dielectric Layer. The dielectric layer of BKKE was obtained by the template prepared by instant sugar and salt particles. The instant sugar and salt granules were mixed in different proportions (1:5, 1:7, 1:9, and 1:11) with a little water and uniformly placed in a hydrophobic surface mold and dried in an oven at 70° C for 1 h. Then, the A and B components of PDMS (SYLGARD 184; Dow Corning) were uniformly mixed in a ratio of 10:1, and the bubbles were removed under vacuum. The PDMS liquid was spin-coated onto the agglomerated instant sugar and salt granules and then covered with another layer of agglomerated sugar and salt template and lightly compacted and cured in an oven at 75 °C for 3 h. Finally, the cured elastomer was placed in an ultrasonic bath for 20 min; the particles were dissolved entirely and dried in an oven.

Fabrication of Capacitive Sensor. The preparation of copper-nickel nanofiber network was based on previous studies in our laboratory.[43] The flexible PET film was directly peeled off from the composite PET film (OKY 200, Bellpet) for use in the electrode portion of the sensor. The BKKE was placed between two flexible electrodes, and the two electrodes were connected to the copper wire for electrical measurement using a conductive silver paste. Finally, the sensor was fixed at the desired test position using Scotch tape (3M).

Characterization and Measurements. The surface characteristics of the Cu/Ni nanowire flexible electrode and BKKE were characterized by field emission SEM (FE-SEM, Hitachi). The sensor's capacitance was measured by an Agilent 4263B LCR meter and NF ZM2372 LCR meter with a set frequency of 1 kHz and a voltage of 1 V. The IMADA force gauge was used to apply pressure to the sensor and record the values. The LabVIEW program simultaneously records the capacitance at different pressures.

■ ASSOCIATED CONTENT

Supporting Information

The Supporting Information is available free of charge on the ACS Publications website at DOI: 10.1021/acsami.9b00941.

Optical photograph image of the Komochi Konbu; schematic illustration describing the formation of the pressure sensor and diagram of PDMS liquid immersion; thickness of the fabricated device; SEM image, 3D map,

DOI: 10.1021/acsami.9b00941
ACS Appl. Mater. Interfaces 2019, 11, 11928−11935

SEM cross-sectional view, and pressure analysis diagram of the bionic Komochi Konbu dielectric layer; comparison of pressure sensors with different dielectric layer; optical photographs of BKKE and mechanism diagram; optical micrograph of BKKE; SEM image of a sensor with solid PDMS as a dielectric layer; capacitive response of a pressure sensor; formula for calculating the bending radius; and signal response of the pressure sensor for single and double-click (PDF)

Video S1 (AVI)

Video S2 (AVI)

AUTHOR INFORMATION

Corresponding Author

*E-mail: shiratori@appi.keio.ac.jp.

ORCID

Seimei Shiratori: 0000-0001-9807-3555

Author Contributions

All authors have given approval to the final version of the manuscript.

Notes

The authors declare no competing financial interest.

ACKNOWLEDGMENTS

We are very grateful to Dr. Hotta Yoshio and Dr. Kyu-Hong Kyung for their help in the experiment, and Dr. Kouji Fujimoto has given many suggestions and comments for this research. This research was partially supported by KLL Ph.D. Program Research Grant. We are also very grateful to SNT Co. and Bell Polyester Products, Inc. for supplying us the OKY 200 flexible Polyester film.

REFERENCES

(1) Gerratt, A. P.; Michaud, H. O.; Lacour, S. P. Elastomeric Electronic Skin for Prosthetic Tactile Sensation. *Adv. Funct. Mater.* **2015**, *25*, 2287−2295.

(2) Zhan, Z.; Lin, R.; Tran, V.-T.; An, J.; Wei, Y.; Du, H.; Tran, T.; Lu, W. Paper/Carbon Nanotube-Based Wearable Pressure Sensor for Physiological Signal Acquisition and Soft Robotic Skin. *ACS Appl. Mater. Interfaces* **2017**, *9*, 37921−37928.

(3) Choong, C.-L.; Shim, M.-B.; Lee, B.-S.; Jeon, S.; Ko, D.-S.; Kang, T.-H.; Bae, J.; Lee, S. H.; Byun, K.-E.; Im, J.; et al. Highly Stretchable Resistive Pressure Sensors Using a Conductive Elastomeric Composite on a Micropyramid Array. *Adv. Mater.* **2014**, *26*, 3451−3458.

(4) Jung, S.; Kim, J. H.; Kim, J.; Choi, S.; Lee, J.; Park, I.; Hyeon, T.; Kim, D.-H. Reverse-Micelle-Induced Porous Pressure-Sensitive Rubber for Wearable Human-Machine Interfaces. *Adv. Mater.* **2014**, *26*, 4825−4830.

(5) Zang, Y.; Zhang, F.; Di, C.-a.; Zhu, D. Advances of Flexible Pressure Sensors toward Artificial Intelligence and Health Care Applications. *Mater. Horiz.* **2015**, *2*, 140−156.

(6) Han, S.-T.; Peng, H.; Sun, Q.; Venkatesh, S.; Chung, K.-S.; Lau, S. C.; Zhou, Y.; Roy, V. A. L. An Overview of the Development of Flexible Sensors. *Adv. Mater.* **2017**, *29*, 1700375.

(7) He, Z.; Elbaz, A.; Gao, B.; Zhang, J.; Su, E.; Gu, Z. Wearable Biosensors: Disposable Morpho Menelaus Based Flexible Microfluidic and Electronic Sensor for the Diagnosis of Neurodegenerative Disease (Adv. Healthcare Mater. 5/2018). *Adv. Healthcare Mater.* **2018**, *7*, 1870025.

(8) Ge, G.; Cai, Y.; Dong, Q.; Zhang, Y.; Shao, J.; Huang, W.; Dong, X. A Flexible Pressure Sensor Based on RGO/Polyaniline Wrapped Sponge with Tunable Sensitivity for Human Motion Detection. *Nanoscale* **2018**, *10*, 10033−10040.

(9) Huynh, T.-P.; Haick, H. Autonomous Flexible Sensors for Health Monitoring. *Adv. Mater.* **2018**, *30*, 1802337.

(10) Ding, Y.; Yang, J.; Tolle, C. R.; Zhu, Z. Flexible and Compressible PEDOT:PSS@Melamine Conductive Sponge Prepared via One-Step Dip Coating as Piezoresistive Pressure Sensor for Human Motion Detection. *ACS Appl. Mater. Interfaces* **2018**, *10*, 16077−16086.

(11) Chen, D.; Pei, Q. Electronic Muscles and Skins: A Review of Soft Sensors and Actuators. *Chem. Rev.* **2017**, *117*, 11239−11268.

(12) Xue, L.; Wang, W.; Guo, Y.; Liu, G.; Wan, P. Flexible Polyaniline/Carbon Nanotube Nanocomposite Film-Based Electronic Gas Sensors. *Sens. Actuators, B* **2017**, *244*, 47−53.

(13) Wang, X.; Liu, Z.; Zhang, T. Flexible Sensing Electronics for Wearable/Attachable Health Monitoring. *Small* **2017**, *13*, 1602790.

(14) Park, D. Y.; Joe, D. J.; Kim, D. H.; Park, H.; Han, J. H.; Jeong, C. K.; Park, H.; Park, J. G.; Joung, B.; Lee, K. J. Self-Powered Real-Time Arterial Pulse Monitoring Using Ultrathin Epidermal Piezoelectric Sensors. *Adv. Mater.* **2017**, *29*, 1702308.

(15) Kim, J.; Kim, N.; Kwon, M.; Lee, J. Attachable Pulse Sensors Integrated with Inorganic Optoelectronic Devices for Monitoring Heart Rates at Various Body Locations. *ACS Appl. Mater. Interfaces* **2017**, *9*, 25700−25705.

(16) Naaz, S.; Poddar, S.; Bayen, S. P.; Mondal, M. K.; Roy, D.; Mondal, S. K.; Chowdhury, P.; Saha, S. K. Tenfold Enhancement of Fluorescence Quantum Yield of Water Soluble Silver Nanoclusters for Nano-Molar Level Glucose Sensing and Precise Determination of Blood Glucose Level. *Sens. Actuators, B* **2018**, *255*, 332−340.

(17) Wang, L.; Jackman, J. A.; Tan, E.-L.; Park, J. H.; Potroz, M. G.; Hwang, E. T.; Cho, N.-J. High-Performance, Flexible Electronic Skin Sensor Incorporating Natural Microcapsule Actuators. *Nano Energy* **2017**, *36*, 38−45.

(18) He, J.; Xiao, P.; Shi, J.; Liang, Y.; Lu, W.; Chen, Y.; Wang, W.; Théato, P.; Kuo, S.-W.; Chen, T. High Performance Humidity Fluctuation Sensor for Wearable Devices via a Bioinspired Atomic-Precise Tunable Graphene-Polymer Heterogeneous Sensing Junction. *Chem. Mater.* **2018**, *30*, 4343−4354.

(19) Nakata, S.; Arie, T.; Akita, S.; Takei, K. Wearable, Flexible, and Multifunctional Healthcare Device with an ISFET Chemical Sensor for Simultaneous Sweat pH and Skin Temperature Monitoring. *ACS Sens.* **2017**, *2*, 443−448.

(20) El Kacimi, A.; Pauliac-Vaujour, E.; Eymery, J. Flexible Capacitive Piezoelectric Sensor with Vertically Aligned Ultralong GaN Wires. *ACS Appl. Mater. Interfaces* **2018**, *10*, 4794−4800.

(21) Wan, S.; Bi, H.; Zhou, Y.; Xie, X.; Su, S.; Yin, K.; Sun, L. Graphene Oxide as High-Performance Dielectric Materials for Capacitive Pressure Sensors. *Carbon* **2017**, *114*, 209−216.

(22) Kang, M.; Kim, J.; Jang, B.; Chae, Y.; Kim, J.-H.; Ahn, J.-H. Graphene-Based Three-Dimensional Capacitive Touch Sensor for Wearable Electronics. *ACS Nano* **2017**, *11*, 7950−7957.

(23) Luo, N.; Huang, Y.; Liu, J.; Chen, S.-C.; Wong, C. P.; Zhao, N. Hollow-Structured Graphene-Silicone-Composite-Based Piezoresistive Sensors: Decoupled Property Tuning and Bending Reliability. *Adv. Mater.* **2017**, *29*, 1702675.

(24) Wu, X.; Ma, Y.; Zhang, G.; Chu, Y.; Du, J.; Zhang, Y.; Li, Z.; Duan, Y.; Fan, Z.; Huang, J. Thermally Stable, Biocompatible, and Flexible Organic Field-Effect Transistors and Their Application in Temperature Sensing Arrays for Artificial Skin. *Adv. Funct. Mater.* **2015**, *25*, 2138−2146.

(25) Ma, Y.; Liu, N.; Li, L.; Hu, X.; Zou, Z.; Wang, J.; Luo, S.; Gao, Y. A Highly Flexible and Sensitive Piezoresistive Sensor Based on MXene with Greatly Changed Interlayer Distances. *Nat. Commun.* **2017**, *8*, 1207.

(26) Pan, L.; Chortos, A.; Yu, G.; Wang, Y.; Isaacson, S.; Allen, R.; Shi, Y.; Dauskardt, R.; Bao, Z. An Ultra-Sensitive Resistive Pressure Sensor Based on Hollow-Sphere Microstructure Induced Elasticity in Conducting Polymer Film. *Nat. Commun.* **2014**, *5*, 3002.

(27) Chen, Z.; Wang, Z.; Li, X.; Lin, Y.; Luo, N.; Long, M.; Zhao, N.; Xu, J.-B. Flexible Piezoelectric-Induced Pressure Sensors for Static

DOI: 10.1021/acsami.9b00941
ACS Appl. Mater. Interfaces 2019, 11, 11928−11935

Measurements Based on Nanowires/Graphene Heterostructures. *ACS Nano* **2017**, *11*, 4507−4513.
(28) Knopfmacher, O.; Hammock, M. L.; Appleton, A. L.; Schwartz, G.; Mei, J.; Lei, T.; Pei, J.; Bao, Z. Highly Stable Organic Polymer Field-Effect Transistor Sensor for Selective Detection in the Marine Environment. *Nat. Commun.* **2014**, *5*, 2954.
(29) Zhu, W.; Deng, Y.; Cao, L. Light-Concentrated Solar Generator and Sensor Based on Flexible Thin-Film Thermoelectric Device. *Nano Energy* **2017**, *34*, 463−471.
(30) Wu, W.; Wang, B.; Segev-Bar, M.; Dou, W.; Niu, F.; Horev, Y. D.; Deng, Y.; Plotkin, M.; Huynh, T.-P.; Jeries, R.; Garaa, A. l.; Badarneh, S.; Chen, L.; Du, M.; Hu, W.; Haick, H. Free-Standing and Eco-Friendly Polyaniline Thin Films for Multifunctional Sensing of Physical and Chemical Stimuli. *Adv. Funct. Mater.* **2017**, *27*, 1703147.
(31) Zhao, S.; Zhu, R. Electronic Skin with Multifunction Sensors Based on Thermosensation. *Adv. Mater.* **2017**, *29*, 1606151.
(32) Liu, S.; Wu, X.; Zhang, D.; Guo, C.; Wang, P.; Hu, W.; Li, X.; Zhou, X.; Xu, H.; Luo, C.; Zhang, J. Ultrafast Dynamic Pressure Sensors Based on Graphene Hybrid Structure. *ACS Appl. Mater. Interfaces* **2017**, *9*, 24148−24154.
(33) Shuai, X.; Zhu, P.; Zeng, W.; Hu, Y.; Liang, X.; Zhang, Y.; Sun, R.; Wong, C.-p. Highly Sensitive Flexible Pressure Sensor Based on Silver Nanowires-Embedded Polydimethylsiloxane Electrode with Microarray Structure. *ACS Appl. Mater. Interfaces* **2017**, *9*, 26314−26324.
(34) Ho, D. H.; Song, R.; Sun, Q.; Park, W.-H.; Kim, S. Y.; Pang, C.; Kim, D. H.; Kim, S.-Y.; Lee, J.; Cho, J. H. Crack-Enhanced Microfluidic Stretchable E-Skin Sensor. *ACS Appl. Mater. Interfaces* **2017**, *9*, 44678−44686.
(35) Nela, L.; Tang, J.; Cao, Q.; Tulevski, G.; Han, S.-J. Large-Area High-Performance Flexible Pressure Sensor with Carbon Nanotube Active Matrix for Electronic Skin. *Nano Lett.* **2018**, *18*, 2054−2059.
(36) Zhang, Y.; Zhang, L.; Cui, K.; Ge, S.; Cheng, X.; Yan, M.; Yu, J.; Liu, H. Flexible Electronics Based on Micro/Nanostructured Paper. *Adv. Mater.* **2018**, *30*, 1801588.
(37) Gong, S.; Schwalb, W.; Wang, Y.; Chen, Y.; Tang, Y.; Si, J.; Shirinzadeh, B.; Cheng, W. A Wearable and Highly Sensitive Pressure Sensor with Ultrathin Gold Nanowires. *Nat. Commun.* **2014**, *5*, 3132.
(38) Cai, S.; Liu, X.; Huang, J.; Liu, Z. Feasibility of Polyethylene Film as Both Supporting Material for Transfer and Target Substrate for Flexible Strain Sensor of CVD Graphene Grown on Cu Foil. *RSC Adv.* **2017**, *7*, 48333−48340.
(39) Su, B.; Gong, S.; Ma, Z.; Yap, L. W.; Cheng, W. Mimosa-Inspired Design of a Flexible Pressure Sensor with Touch Sensitivity. *Small* **2015**, *11*, 1886−1891.
(40) Atalay, O.; Atalay, A.; Gafford, J.; Walsh, C. A Highly Sensitive Capacitive-Based Soft Pressure Sensor Based on a Conductive Fabric and a Microporous Dielectric Layer. *Adv. Mater. Technol.* **2018**, *3*, 1700237.
(41) He, Z.; Chen, W.; Liang, B.; Liu, C.; Yang, L.; Lu, D.; Mo, Z.; Zhu, H.; Tang, Z.; Gui, X. Capacitive Pressure Sensor with High Sensitivity and Fast Response to Dynamic Interaction Based on Graphene and Porous Nylon Networks. *ACS Appl. Mater. Interfaces* **2018**, *10*, 12816−12823.
(42) Song, Y.; Chen, H.; Su, Z.; Chen, X.; Miao, L.; Zhang, J.; Cheng, X.; Zhang, H. Highly Compressible Integrated Supercapacitor-Piezoresistance-Sensor System with CNT-PDMS Sponge for Health Monitoring. *Small* **2017**, *13*, 1702091.
(43) Yoshikawa, R.; Tenjimbayashi, M.; Matsubayashi, T.; Manabe, K.; Magagnin, L.; Monnai, Y.; Shiratori, S. Designing a Flexible and Transparent Ultrarapid Electrothermogenic Film Based on Thermal Loss Suppression Effect: A Self-Fused Cu/Ni Composite Junctionless Nanonetwork for Effective Deicing Heater. *ACS Appl. Nano Mater.* **2018**, *1*, 860−868.